HHS Public Access

Author manuscript

Hepatology. Author manuscript; available in PMC 2018 September 01.

Published in final edited form as:

Hepatology. 2017 September ; 66(3): 869–884. doi:10.1002/hep.29145.

The role of LncRNA H19 in gender disparity of cholestatic liver injury in Mdr2$^{-/-}$ mice

Xiaojiaoyang Li[1,2], **Runping Liu**[2,3], **Jing Yang**[1,2], **Lixin Sun**[1,2], **Luyong Zhang**[1,3], **Zhenzhou Jiang**[1], **Puneet Puri**[4], **Emily C. Gurley**[2], **Guanhua Lai**[5], **Yuping Tang**[6], **Zhiming Huang**[7], **William M Pandak**[2,4], **Phillip B. Hylemon**[2,4], and **Huiping Zhou**[2,4,7]

[1]Jiangsu Key Laboratory of Drug Screening, China Pharmaceutical University, Nanjing, Jiangsu, China

[2]Department of Microbiology and Immunology and McGuire Veterans Affairs Medical Center

[3]Guangdong Pharmaceutical University, Guangzhou, China

[4]Department of Internal Medicine/GI Division, Virginia Commonwealth University, Richmond, Virginia, 23298

[5]Department of Pathology, Medical College of Virginia Campus, Virginia Commonwealth University, Richmond, Virginia, 23298

[6]Jiangsu Collaborative Innovation Center of Chinese Medicinal Resource Industrialization and Jiangsu Key Laboratory for High Technology Research of TCM Formulae, Nanjing University of Traditional Chinese Medicine, Nanjing, China

[7]Department of Gastroenterology, The First Affiliated hospital of Wenzhou Medical University, Wenzhou, China

Abstract

The multi-drug resistance 2 knockout (Mdr2$^{-/-}$) mouse is a well-established model of cholestatic cholangiopathies. Female Mdr2$^{-/-}$ mice develop more severe hepatobiliary damage than male Mdr2$^{-/-}$ mice, which is correlated with a higher proportion of taurocholate (TCA) in bile. Although estrogen has been identified as an important player in intrahepatic cholestasis, the underlying molecular mechanisms of gender-based disparity of cholestatic injury remain unclear. The long non-coding RNA H19 is an imprinted, maternally expressed and estrogen-targeted gene, which is significantly induced in human fibrotic/cirrhotic liver and bile duct ligated mouse liver. However, whether aberrant expression of H19 accounts for gender-based disparity of cholestatic injury in Mdr2$^{-/-}$ mice remains unknown. The current study demonstrated that H19 was markedly

Address correspondence to: Huiping Zhou, Ph.D, Department of Microbiology & Immunology, Virginia Commonwealth University, McGuire Veterans Affairs Medical Center, P.O. Box 980678, Richmond, VA 23298-0678, Tel: 804-828-6817; Fax: 804-828-0676, huiping.zhou@vcuhealth.org; Luyong Zhang, Ph.D, Jiangsu Key Laboratory of Drug Screening, China Pharmaceutical University, Nanjing, Jiangsu, China, Tel: 86-25-83271500; Fax: 86-25-83271500, lyzhang@cpu.edu.cn.

Contributions: LX and HZ conceived the original ideas, designed the study, analyzed the data and wrote the manuscript; RL, JY and LS carried out the real-time PCR analysis, measurement of serum and liver bile acids, ALT, AST, ALP and hydroxyproline analysis, Western blot analysis, immunohistochemistry and data analysis. LS did immunohistochemistry. GL helped by doing histology analysis. ECG did animal breeding and genotyping. PBH, PP, WMP, YT and ZH helped data analysis and review manuscript.

Competing Financial interest: The authors declare no competing financial interest.

induced (~200-fold) in the livers of female Mdr2$^{-/-}$ mice at advanced stages of cholestasis (100-day-old), but not in aged-matched male Mdr2$^{-/-}$ mice. During the early stages of cholestasis, H19 expression was minimal. We further determined that the hepatic H19 was mainly expressed in cholangiocytes, not hepatocytes. Both TCA and estrogen significantly activated the ERK1/2 signaling pathway and induced H19 expression in cholangiocytes. Knocking down H19 not only significantly reduced TCA/estrogen-induced expression of fibrotic genes and sphingosine 1-phosphate receptor 2 (S1PR2) in cholangiocytes, but also markedly reduced cholestatic injury in female Mdr2$^{-/-}$ mice. Furthermore, the expression of small heterodimer partner was substantially inhibited at advanced stages of liver fibrosis, which was reversed by H19 shRNA in female Mdr2$^{-/-}$ mice. Similar findings were obtained in human PSC liver samples.

Conclusion—H19 plays a critical role in the disease progression of cholestasis and represents a key factor that causes the gender disparity of cholestatic liver injury in Mdr2$^{-/-}$ mice.

Keywords

H19; TCA; estrogen; cholangiocyte; cholestasis

Introduction

Development of a biliary fibrosis mouse model, by deletion of the canalicular phospholipid flippase (Mdr2$^{-/-}$), has provided a very useful tool to study the disease pathology of chronic biliary liver disease and test potential therapeutics (1, 2). Interestingly, previous studies found that female Mdr2$^{-/-}$ mice developed more severe cholestatic liver injury with a more hydrophobic bile acid pool composition and higher levels of taurocholate (TCA) in the bile when compared to their male counterparts (3). Although it is well known that female hormones play a critical role in the induction of cholestatic injury, the underlying cellular/molecular mechanisms accounting for the gender disparity of cholestatic liver injury remain to be determined (4–6).

Our previous studies reported that conjugated bile acids, especially TCA, promote invasive growth of cholangiocarcinoma *via* activation of sphingosine 1-phosphate receptor 2 (S1PR2) and up-regulation of cyclooxygenase 2 (COX2) (7, 8). Recently, we determined that the S1PR2-mediated signaling pathway is also involved in bile duct ligation (BDL)-induced cholestasis and fibrosis (Hepatology, under revision). TCA was also shown to be involved in estrogen-induced cholestasis (9). These observations suggest that both TCA- and estrogen-mediated signaling pathways may contribute to the gender-disparity of cholestatic liver injury.

The long non-coding RNA (LncRNA) H19 is an imprinted and a maternally expressed gene. It is one of a few LncRNAs conserved between human and mouse and plays a key role in the regulation of cell proliferation and differentiation (10). H19 is also an estrogen-regulated transcript and aberrant expression of H19 has been associated with cell proliferation and migration in a variety of cancers, including gastric, gallbladder and pancreatic cancer (11, 12). It is also up-regulated in animal models of CCl_4-induced cirrhosis and BDL-induced fibrosis (13,14). However, there is a gap in our knowledge about the mechanism by which

bile acids and estrogen-mediated signaling regulates H19 expression, and the role of H19 in gender disparity of cholestatic liver injury in Mdr2$^{-/-}$ mice remains unknown.

In the present study, we report that H19 is predominantly expressed in cholangiocytes and aberrant expression of H19 was correlated with the progression of fibrotic liver injury in female Mdr2$^{-/-}$ mice. These findings suggest that the TCA/S1PR2- and estrogen-induced signaling pathways along with H19 play key roles in cholestatic liver injury.

Materials and Methods

Materials

Detailed information of all chemicals and reagents used in this study is provided online in the supplementary information.

Animal Studies

FVB wild-type mice (both male and female) were purchased from Jackson Laboratories (Bar Harbor, ME). Mdr2 knockout mice (Mdr2$^{-/-}$) were gifts from Dr. Gianfranco Alpini (Texas A&M HSC College of Medicine). The mice were housed under 12h light/12 dark cycle and fed standard chow and tap water *ad libitum*. Mice at different ages (60, 100 and 180 days) were used in this study. At the end of the experiment, mice were weighed and sacrificed. Blood and bile were collected to measure liver functional enzyme activities and bile acid and hydroxyproline concentrations. Livers were harvested and either fixed and processed for histological analysis or frozen in liquid nitrogen and stored at −80°C for further analysis. For the *in vivo* knockdown of H19 experiment, female Mdr2$^{-/-}$mice (60 days) were injected with purified adenovirus (2×10^{10} virus particles per mouse) *via* tail vein. After 7 days, mice were harvested as described above. All animal study protocols were approved by the Institutional Animal Care and Use Committee of Virginia Commonwealth University. In addition, all experiments were performed in accordance with institutional guidelines and regulations.

Human liver samples

Frozen PSC patient liver tissues and normal human liver tissues from age were obtained through the Liver Tissue Cell Distribution System (LTCDS) (Minneapolis, Minnesota), which was funded by NIH Contract# HSN276201200017C.

Measurement of the liver functional enzyme activities, hydroxyproline and total bile acid levels

Serum levels of alkaline phosphatase (ALP), aspartate aminotransferase (AST), alanine aminotransferase (ALT) and hydroxyproline were measured using commercially available assay kits from Sigma (St. Louis, MO) according to the manufacturer's instruction. Total bile acid (TBA) was measured by an assay kit from Crystal Chem (Downers Drive, IL). Liver samples were homogenized in RIPA buffer and total protein lysates were used for analysis. Results were normalized with total protein amount. The absorptions were determined by the Victor3 Multilabel Plate Counter from PerkinElmer (Waltham, MA).

All other methods were described in online supplementary file.

Results

Gender disparity of cholestatic liver injury in Mdr2$^{-/-}$ mice

We first compared the cholestatic liver injury in age-matched male and female WT (WT) and Mdr2$^{-/-}$ mice. As shown in Fig. 1A, serum alkaline phosphatase (ALP) and bile acid levels were dramatically increased in 100-day-old Mdr2$^{-/-}$ mice compared to those in aged matched WT mice, especially in female Mdr2$^{-/-}$ mice. Similarly, the hepatic ALP and bile acid levels were also increased significantly Mdr2$^{-/-}$ mice (Supplementary Fig. 1A). Although the serum levels of alanine aminotransferase (ALT) and aspartate aminotransferase (AST) were increased in Mdr2$^{-/-}$ mice compared to WT mice, there was no significant difference between male and female Mdr2$^{-/-}$ mice (Supplementary Fig. 1B). In addition, the ratios of liver or spleen weight over body weight of female Mdr2$^{-/-}$ mice were increased compared to their male counterparts (Supplementary Fig. 1C). Histological analysis revealed that female Mdr2$^{-/-}$ mice had more severe cholestatic liver injury as illustrated by H&E and Masson's Trichrome staining (Fig. 1B). Real-time PCR analysis showed that mRNA steady-state level of collagen I was significantly increased in female Mdr2$^{-/-}$ mice, but not in male Mdr2$^{-/-}$ mice (Fig. 1C). Consistently, the hepatic hydroxyproline level was increased in female Mdr2$^{-/-}$ mice, but not in male Mdr2$^{-/-}$ mice (Fig. 1D). In addition, both real-time RT-PCR and Western blot analysis showed increased levels of PCNA in the livers of female Mdr2$^{-/-}$ mice (Supplementary Fig. 1D) and (Fig. 1E). Immunohistochemistry staining further showed significant increase of PCNA and CK-19 expression in female Mdr2$^{-/-}$ mice, indicating ductal proliferation and increase of bile duct mass (Fig. 1F and Supplementary Fig. 1E). Furthermore, the expression of several inflammatory mediators (IL-6, TNF-α, CXCL10, CCL17 and CCL22) were also largely increased in female Mdr2$^{-/-}$ mice, while male Mdr2$^{-/-}$ mice had a slight or no increase when compared to gender-matched WT mice (Supplementary Fig. 1F).

To further determine if the gender disparity of biliary fibrosis is dependent on the age, we compared younger Mdr2$^{-/-}$ mice (60-day-old) with older ones (100-day-old). As shown in Fig. 2A–B, 60-day-old male Mdr2$^{-/-}$ mice only developed mild biliary cholestatic injury, but 100-day-old female Mdr2$^{-/-}$ mice developed significant cholestatic injury as indicated by an increase in serum ALP and total bile acid levels (Fig. 2A) and fibrosis as indicated by H&E staining and Masson's Trichrome staining (Fig. 2B). Real-time PCR analysis indicated that there was no significant difference of Ki67 mRNA levels between male and female Mdr2$^{-/-}$ mice at 60 days age, but Ki67 mRNA expression was much higher in female Mdr2$^{-/-}$ mice than male Mdr2$^{-/-}$ mice at 100 days of age (Fig. 2C). Although no significant change was observed in the PCNA mRNA levels between 60-day-old male and female Mdr2$^{-/-}$ mice, the protein levels of PCNA were significantly up-regulated (Fig. 2D–E). For 100-day-old Mdr2$^{-/-}$ mice, PCNA mRNA and protein levels were both significantly increased in female and male mice. No significant changes in the AST and ALT levels were detected (Supplementary Fig. 2A). The ratios of liver or spleen weight over the body weight and the mRNA levels of inflammatory mediators were similar between 60-day-old male and female Mdr2$^{-/-}$ mice, but TNF-α, CXCL10 and CCL17 were significantly upregulated in

100-day-old female Mdr2$^{-/-}$ mice (Supplementary Fig. 2B–D). Immunohistochemistry staining also showed significant increase in PCNA and CK-19 expression in 60-day-old female Mdr2$^{-/-}$ mice, which was more pronounced in 100-day-old female Mdr2$^{-/-}$ mice (Fig. 2F and Supplementary Fig. 2E).

Aberrant expression of H19 is correlated with the severity of biliary fibrosis in female Mdr2$^{-/-}$ mice

LncRNA H19 is an estrogen-regulated gene whose expression is suppressed in adult liver (13–15). The aberrant expression of H19 has been associated with various cancers (10, 12, 16–19). H19 is also up-regulated in BDL-mice (15). To identify the role of H19 in the development of biliary fibrosis in Mdr2$^{-/-}$ mice, we first examined the expression of hepatic H19 in WT and Mdr2$^{-/-}$ mice. As shown in Fig. 3A, the expression of hepatic H19 in 100-day-old WT mice was very low with a slight but significant increase in male Mdr2$^{-/-}$ mice. In contrast, there was a striking 200-fold increase in hepatic H19 expression in female Mdr2$^{-/-}$ mice. To further determine whether hepatic H19 expression was correlated to the fibrotic progression seen in female Mdr2$^{-/-}$ mice, we compared hepatic H19 expression levels in 60-day-old Mdr2$^{-/-}$ mice with that in 100-day-old Mdr2$^{-/-}$ mice. As shown in Fig. 3B, at 60 days old, the hepatic H19 levels were 6-fold higher in female Mdr2$^{-/-}$ mice than that in male Mdr2$^{-/-}$ mice, but at 100 days old, hepatic H19 levels were more than 20-fold higher in the female Mdr2$^{-/-}$ mice.

A previous study has reported that c-Myc induced H19 expression by allele-specific binding (20). As shown in Fig. 3C, the expression levels of c-Myc were significantly increased in 100-day-old female Mdr2$^{-/-}$ mice compared to age-matched WT mice. However, there was no significant difference between 60-day and 100-day-old female Mdr2$^{-/-}$ mice (Fig. 3D). Recently, it was reported that hepatic overexpression of Bcl-2 induced expression of H19 and rapid SHP protein degradation *via* the activation of caspase-8 pathway in WT mice (15). However, the expression of Bcl-2 in female Mdr2$^{-/-}$ mice only increased slightly, and no change was observed in male Mdr2$^{-/-}$ mice (Supplementary Fig. 3A–D). In addition, the protein expression levels of the FXRα and SHP were significantly down-regulated in 100-day-old Mdr2$^{-/-}$ mice when compared to those in 60-day-old Mdr2$^{-/-}$ mice (Fig. 3E), but not the mRNA levels (Supplementary 3E–F). Moreover, the expression level of H19 was dramatically increased in older female Mdr2$^{-/-}$ mice, which was accompanied by a significant down-regulation of SHP at 180 days (Supplementary Fig. 4A–B). The expression levels of ki67, PCNA and collagen I were markedly upregulated in both 100-day and 180-day-old female mice (Supplementary Fig. 4C–E). The mRNA levels of Bcl-2 were mildly increased in female Mdr2$^{-/-}$ mice both at 100-day and 180-day-old (Supplementary Fig. 4F). These results suggest that Bcl-2 plays a minimal role in the up-regulation of H19 and down-regulation of SHP in aged female Mdr2$^{-/-}$ mice.

Bile acid receptors and cholestatic injury in Mdr2$^{-/-}$ mice

A recent study reported that G-protein coupled receptor (GPCR) TGR5 is required for bile acid-induced cholangiocyte proliferation in BDL models (21). However, both in BDL mice and Mdr2$^{-/-}$ mice, the most abundant bile acids accumulated in the liver are conjugated primary bile acids, which are weak agonists of TGR5 (3). Our previous studies reported that

TCA activates the S1PR2 in both hepatocytes and cholangiocytes (7, 19, 22). TGR5 is expressed in non-parenchymal cells of liver, such as Kupffer cells and cholangiocytes, but not expressed in hepatocytes (21). Recently, we reported that the expression level of S1PR2 in cholangiocytes was much higher than that of TGR5, and S1PR2 null mice were protected from BDL-induced hepatic biliary injury (23). To determine whether S1PR2 plays a role in the up-regulation of H19 and cholestatic liver injury in female Mdr2$^{-/-}$ mice, we first determined the mRNA levels of S1PR2. As shown in Fig. 4A, hepatic S1PR2 was significantly up-regulated in both male and female Mdr2$^{-/-}$ mice when compared to WT mice, especially in female Mdr2$^{-/-}$ mice. Also, compared to 60-day-old female mice, 100-day-old female mice showed much higher levels of S1PR2 mRNA (Fig. 4B). However, the hepatic mRNA levels of TGR5 were not significantly different between WT and Mdr2$^{-/-}$ mice (Supplementary Fig. 5A–B). There was also no gender difference in TGR5 expression in Mdr2$^{-/-}$ mice. We recently reported that S1PR2 is the predominant S1PR in cholangiocytes (Hepatology, under revision). To further compare the expression levels in different types of hepatic cells, we isolated the primary hepatocytes, cholangiocytes and Kupffer cells from WT and Mdr2$^{-/-}$ mice. As shown in Fig. 4C, S1PR2 was highly expressed in cholangiocytes from both male and female Mdr2$^{-/-}$ mice and significantly up-regulated in hepatocytes and Kupffer cells from female Mdr2$^{-/-}$ mice.

It is well known that estrogen induces cholestatic liver injury by activating estrogen receptor α (ERα), the major isoform expressed in the liver (24). To determine whether the estrogen level was correlated to cholestatic liver injury in female Mdr2$^{-/-}$ mice, we measured serum estradiol levels using an ELISA kit. As shown in Supplementary Fig. 5C, the estradiol levels were significantly increased in aged female Mdr2$^{-/-}$ mice (100-day and 180-day-old). ERα expression was higher in female mice (both WT and Mdr2$^{-/-}$ mice) than that in male mice (Supplementary Fig. 5D). Although ERα is also expressed in cholangiocytes and Kupffer cells, the expression level was lower than that in hepatocytes (Supplementary Fig. 5E). Also, there was no significant difference of ERα expression in hepatocytes and cholangiocytes between WT and Mdr2$^{-/-}$ mice, but Kupffer cells from female Mdr2$^{-/-}$ mice had higher ERα levels compared to WT mice. Furthermore, H19 expression was strikingly up-regulated in the hepatocytes and cholangiocytes from female Mdr2$^{-/-}$ mice, especially in cholangiocytes (Fig. 4D).

Effect of TCA and estrogen on H19 expression

Our previous studies showed that bile acids and estrogen activated ERK1/2 and AMPK signaling pathways in hepatocytes and cholangiocarcinoma cells (6–8, 22). We further determined whether the ERK1/2 signaling pathway was involved in TCA- and 17β-Estradiol (E2)-mediated up-regulation of H19 using cultured mouse large cholangiocytes (MLE). As shown in Fig. 5A–B, TCA rapidly induced ERK1/2 activation, while E2 had a delayed response. Both TCA and E2 activated AMPK. In addition, both TCA and E2 up-regulated H19 expression without an additive or synergistic effect (Fig. 5C). By using a chemical inhibitor of MAPK (U0126) and chemical antagonists of S1PR2 and ERα (JTE-013 and ICI182,780, respectively), we found that both TCA and E2-induced H19 expression was blocked by U0126 as well as their corresponding antagonists (Fig. 5C). In addition, both TCA and E2 significantly up-regulated α-SMA, but both had no effect on Bcl-2 or Collagen

I mRNA levels. Co-treatment with TCA and E2 significantly increased mRNA levels of Bcl-2, α-SMA and Collagen I, which was inhibited by U0126, a combination of JTE-013 and ICI182, 780 (Fig. 5C–E) as well as by a specific shRNA of H19 (Fig. 6A–D). Down-regulation of H19 had no effect on FXR mRNA levels (data not shown), but slightly up-regulated SHP mRNA expression in MLE cells (Fig. 6E). However, H19 shRNA significantly blocked TCA-induced expression of S1PR2 in cholangiocytes (Fig. 6F)

H19 knockdown alleviated cholestatic liver injury in female Mdr2$^{-/-}$ mice

To further define the crucial role of H19 in cholestatic and fibrotic liver injury in female Mdr2$^{-/-}$ mice, the adenovirus of H19 shRNA or control shRNA was injected *via* tail vein to knockdown the expression of H19 in female Mdr2$^{-/-}$ mice. As shown in Fig. 7A, down-regulation of H19 in female Mdr2$^{-/-}$ mice significantly reduced serum ALP and total bile acid levels, but had no effect on ALT and AST (Supplementary Fig. 6). Histological analysis further showed that down-regulation of H19 markedly reduced hepatobiliary injury and fibrosis (Fig. 7B). A previous study reported that overexpression of Bcl-2 induced rapid protein degradation of SHP (15). However, there was no significant difference of Bcl-2 protein levels between 60-day and 100-day-old female Mdr2$^{-/-}$ mice (Supplementary Fig. 3D), while SHP protein level in 100-day-old female Mdr2$^{-/-}$ mice was strikingly low compared to that in 60-day-old female Mdr2$^{-/-}$ mice (Fig. 3E). As shown in Fig. 7C–D, H19-shRNA effectively down-regulated hepatic H19 levels and increased SHP mRNA (~1.5 fold) and dramatically up-regulated SHP protein levels, which was accompanied by down-regulation of Cyp7A1 expression (Supplementary Fig. 7A). In addition, H19 knockdown in female Mdr2$^{-/-}$ mice also decreased Bcl-2, c-Myc, S1PR2, ERα and PCNA expression, but had no effect on FXR expression (Fig. 7C–D and Supplementary Fig. 7C). Immunohistochemistry analysis of PCNA and CK-19 further showed that cholangiocyte proliferation was inhibited by H19 shRNA (Fig. 7E and Supplementary Fig. 7D). Furthermore, H19 knockdown significantly reduced the mRNA levels of Ntcp and ABCG8, but induced the expression of Ostα, suggesting a reduction of bile acid and cholesterol accumulation in hepatocytes (Supplementary Fig. 7E–F).

Aberrant expression of H19 in female PSC patients

To further determine whether our findings in female Mdr2$^{-/-}$ mice translational impact on human PSC patients, we obtained frozen sex-matched PSC patient and human normal liver tissues from NIH-sponsored LTDCS. The real-time PCR results showed similar expression patterns of H19, c-Myc, Ki67, Collagen I, FXRs, SHP and S1PR2 observed in Mdr2$^{-/-}$ mice (Supplementary Fig. 8). Interestingly, S1PR2 were significantly up-regulated in all PSC patients, especially in female PSC patients.

Discussion

Mdr2$^{-/-}$ mice have been widely used as a cholestatic biliary disease animal model, which recapitulates the Mdr3 mutation-related hepatobiliary diseases in humans (25). Interestingly, female Mdr2$^{-/-}$ mice showed more severe cholestatic and fibrotic symptoms than their male counterparts, as evidenced by increased hepatic bile acids and fibrosis (26, 27). Previous studies reported that the gender difference in injury in Mdr2$^{-/-}$ mice was mainly due to the

different requirement for bile acid and phospholipid secretion between female and male mice (28). Furthermore, female Mdr2$^{-/-}$ mice showed a higher proportion of TCA in bile salt pool composition than male Mdr2$^{-/-}$ mice, which was also regarded as a potential cause of gender difference in fibrotic injury (3, 27). These studies suggest that both conjugated bile acids, mainly TCA, and estrogen both play a critical role in gender disparity of cholestatic injury in Mdr2$^{-/-}$ mice. However, the cellular/molecular mechanisms were unclear. In the present study, we identified, for the first time, that LncRNA H19 is instrumental in TCA- and estrogen-induced cholestatic injury in female Mdr2$^{-/-}$ mice.

It is well recognized that bile acids are important signaling molecules and play important roles in regulating lipid, glucose and energy metabolisms (19, 29, 30). In the BDL-induced cholestatic model, the levels of conjugated bile acids were significantly increased both in liver and serum (31). We previously demonstrated that TCA-mediated activation of S1PR2 is responsible for the activation of ERK1/2 and AKT signaling pathways in primary hepatocytes (22) and invasive growth of cholangiocarcinoma cells (7, 8). Our most recent studies reported that S1PR2 plays a critical role in BDL-induced cholestatic injury (23). In the current study, we also found that hepatic S1PR2 expression was significantly up-regulated in Mdr2$^{-/-}$ mice during progression of hepatic fibrosis (Fig. 4). We further showed that the expression level of S1PR2 in primary hepatocytes isolated from female mice was significantly higher than that from male mice both in WT and Mdr2$^{-/-}$ mice, but there was no significant gender difference in cholangiocytes. There is increasing evidence indicating that dysregulation of bile acid-mediated signaling pathways contributes to cholestatic liver diseases. Recently, it was reported that TGR5 is an important mediator of bile acid-induced cholangiocyte proliferation *in vivo* and *in vitro* (21). It also has been reported that a dual FXR/TGR5 agonist, INT-767, significantly reduced hepatic inflammation and biliary fibrosis in Mdr2$^{-/-}$ male mice, whereas a single agonist of FXR and TGR5 (INT-747 and INT-777, respectively) had no hepatoprotective effects (32). However, the current study indicates that the TGR5 expression levels are similar in both male and female Mdr2$^{-/-}$ mice (Supplementary Fig. 5). It has been reported that TGR5 is mainly activated by secondary bile acids and conjugated primary bile acids are weak agonists of TGR5 (33). Although TGR5 is expressed in cholangiocytes, its expression level is much lower compared to that of S1PR2. In addition, the most abundant bile acids accumulated in the liver of Mdr2$^{-/-}$mice are conjugated primary bile acids, and female Mdr2$^{-/-}$ mice have a higher proportion of TCA in the bile (3). Therefore, S1PR2 may play a more crucial role than TGR5 in the gender disparity of cholestatic injury in Mdr2$^{-/-}$ mice.

LncRNAs have important biological functions, and H19 is one of the few well-characterized lncRNA. Aberrant expression of H19 has been linked to various disease states (19, 34). However, little is known about the role of H19 in cholestatic liver injury, especially in estrogen-mediated cholestasis. The current study indicates that H19 is a key player in promoting cholestatic injury in female Mdr2$^{-/-}$ mice. The expression level of H19 was dramatically up-regulated in cholangiocytes from female Mdr2$^{-/-}$ mice (Fig. 4). Estrogen has been well studied as a pro-cholestatic agent both *in vitro* cell culture and *in vivo* animal models (35). We recently reported that estrogen-induced activation of cAMP-ERK1/2-LKB1-AMPK signaling pathways contributed to suppression of FXRα expression in hepatocytes, resulting in disruption of bile acid homeostasis (6). While ER expression is

relatively low in cholangiocytes under normal physiological conditions, its expression was however markedly increased in proliferating cholangiocytes (5, 36). In the current study, we found that the mRNA levels of hepatic ERα are similar between WT and Mdr2$^{-/-}$ female mice (Supplementary Fig. 5C). In contrast, the S1PR2 mRNA levels are markedly increased in Mdr2$^{-/-}$ female mice (Fig. 4). Interestingly, in cultured mouse cholangiocytes, both E2- and TCA-induced up-regulation of H19 is inhibited by the MAPK inhibitor, U0126 (Fig. 5C). Our unpublished studies indicated that knockdown S1PR2 in Mdr2$^{-/-}$ mice significantly reduced hepatic H19 expression and fibrotic injury (data not shown). These findings suggest that TCA/S1PR2- and estrogen/ER-mediated activation of ERK1/2 signaling pathway and subsequent upregulation of H19 represents a key event promoting cholestatic injury in female Mdr2$^{-/-}$ mice. Furthermore, our findings in human PSC patients (Supplementary Fig. 8) indicate that Mdr2$^{-/-}$ mice are suitable model for PSC. The gender disparity of cholestatic injury in Mdr2$^{-/-}$ mice can be translated to PSC in human patients.

A recent study reported that adenovirus-mediated gene hepatic overexpression of Bcl-2 caused severe liver injury, fibrosis and inflammation, which were accompanied by a significant induction of H19 and rapid SHP protein degradation *via* activation of the caspase-8 signaling pathway (15). In our current study, we did not find significant differences of Bcl-2 expression levels between female WT and Mdr2$^{-/-}$ mice. It was demonstrated that Bcl-2 expression has no correlation to the H19 expression and severity of hepatic fibrotic injury (Supplementary Fig. 3). However, S1PR2 expression was significantly up-regulated during progression of fibrosis and correlated to aberrant expression of H19 (Fig. 4). In addition, our results indicate that SHP protein levels are inversely related to H19 expression levels. Down-regulation of H19 *in vivo* strikingly up-regulated SHP expression both at mRNA and protein levels (Fig. 7C–D). Since SHP is mainly expressed in hepatocytes, while H19 is mainly expressed in cholangiocytes, how SHP expression is regulated by H19 remains to be determined. Our preliminary studies may suggest that cell-cell communication *via* extracellular vesicles may contribute to cross-talk between hepatocytes and cholangiocytes.

H19 has been identified not only as an estrogen-regulated gene but also a c-Myc-targeted gene (20). Binding of c-Myc to evolutionarily conserved E-boxes near the imprinting control region of the H19 promoter facilitates histone acetylation and transcriptional initiation. Our current study indicates that c-Myc is significantly up-regulated in female Mdr2$^{-/-}$ mice (Fig. 3C–D). However, its expression level is not correlated to the severity of cholestatic injury. Although there is more severe hepatic injury in 100-day female Mdr2$^{-/-}$ mice compared to 60-day female Mdr2$^{-/-}$mice, the c-Myc protein levels are similar (Fig. 3D). In contrast, the H19 expression level is closely correlated to hepatic fibrotic injury. Down regulation of H19 also mildly reduces hepatic c-Myc expression (Fig. 7D). These results suggest that c-Myc-independent regulation of H19 expression plays a critical role in cholestatic injury in female Mdr2$^{-/-}$ mice. Furthermore, consistent with our previous finding (19), upregulation of hepatic S1PR2 was also correlated to the increased protein level of sphingosine kinase 2 (SphK2) in female Mdr2$^{-/-}$mice, which was blocked by H19 shRNA (Supplementary Fig. 9).

In summary, based on our findings from previous and current studies, we propose that both TCA-mediated activation of S1PR2 and estrogen-induced activation of ER induce subsequent activation of ERK1/2, which is responsible for upregulation of H19 and SphK2 in cholangiocytes (Fig. 8). The cross-talk between hepatocytes and cholangiocytes *via* extracellular vesicles results in suppression of SHP expression and disruption of bile acid homeostasis and eventually hepatic cholestatic injury. H19 is central player in the gender related disparity of cholestatic injury in Mdr2$^{-/-}$ mice and represents a potential therapeutic target for cholestatic diseases.

Supplementary Material

Refer to Web version on PubMed Central for supplementary material.

Acknowledgments

This work was supported by National Institutes of Health Grant R01 DK104893 (to HZ and PBH), R01DK-057543 (to PBH and HZ), VA Merit Award I01BX001390 (to HZ); NIAAA K23 AA021179 to PP; National Natural Science Foundation of China Grants 81320108029 (to LZ.), 81070245 and 81270489 (to H.Z.); Massey Cancer Center pilot grant (to HZ and PBH). Microscopy was performed at the VCU Microscopy Facility, supported in part by funding from NIH-NCI Cancer Center Grant P30 CA016059. Specific Fund for Public Interest Research of Traditional Chinese Medicine, Ministry of Finance, China (201507004-002). National “Major Scientific and Technological Special Project for Significant New Drugs Creation” Project (2015ZX09501004-002-004).

Abbreviations

Mdr2$^{-/-}$ mice	multidrug resistance 2 gene knockout mice
TCA	taurocholate
S1PR2	sphingosine 1-phosphate receptor 2
SHP	small heterodimer partner
COX2	cyclooxygenase 2
BDL	bile duct ligation
LncRNA	long non-coding RNA
ALP	alkaline phosphatase
ALT	alanine transaminase
AST	aspartate transaminase
GPCR	G protein coupled receptor
ER	estrogen receptor
E2	17β-Estradiol
MLE	mouse large cholangiocyte
ERK1/2	extracellular signal-regulated kinase 1/2

AMPK	AMP-activated protein kinase
FXR	farnesoid X receptor
TBA	total bile acid

References

1. Smit JJ, Schinkel AH, Oude Elferink RP, Groen AK, Wagenaar E, van Deemter L, Mol CA, et al. Homozygous disruption of the murine mdr2 P-glycoprotein gene leads to a complete absence of phospholipid from bile and to liver disease. Cell. 1993; 75:451–462. [PubMed: 8106172]
2. Popov Y, Patsenker E, Fickert P, Trauner M, Schuppan D. Mdr2 (Abcb4)−/− mice spontaneously develop severe biliary fibrosis via massive dysregulation of pro- and antifibrogenic genes. J Hepatol. 2005; 43:1045–1054. [PubMed: 16223543]
3. van Nieuwerk CM, Groen AK, Ottenhoff R, van Wijland M, van den Bergh Weerman MA, Tytgat GN, Offerhaus JJ, et al. The role of bile salt composition in liver pathology of mdr2 (−/−) mice: differences between males and females. J Hepatol. 1997; 26:138–145. [PubMed: 9148004]
4. Williamson C, Geenes V. Intrahepatic Cholestasis of Pregnancy. Obstetrics & Gynecology. 2014; 124:120–133. [PubMed: 24901263]
5. Alvaro D, Alpini G, Onori P, Perego L, Svegliata Baroni G, Franchitto A, Baiocchi L, et al. Estrogens stimulate proliferation of intrahepatic biliary epithelium in rats. Gastroenterology. 2000; 119:1681–1691. [PubMed: 11113090]
6. Li X, Liu R, Luo L, Yu L, Chen X, Sun L, Wang T, et al. Role of AMP-activated protein kinase alpha1 in 17alpha-ethinylestradiol-induced cholestasis in rats. Arch Toxicol. 2016; 91:481–494. [PubMed: 27090119]
7. Liu R, Zhao R, Zhou X, Liang X, Campbell DJ, Zhang X, Zhang L, et al. Conjugated bile acids promote cholangiocarcinoma cell invasive growth through activation of sphingosine 1-phosphate receptor 2. Hepatology. 2014; 60:908–918. [PubMed: 24700501]
8. Liu R, Li X, Qiang X, Luo L, Hylemon PB, Jiang Z, Zhang L, et al. Taurocholate Induces Cyclooxygenase-2 Expression via the Sphingosine 1-phosphate Receptor 2 in a Human Cholangiocarcinoma Cell Line. J Biol Chem. 2015; 290:30988–31002. [PubMed: 26518876]
9. Alvaro D, Mancino MG, Onori P, Franchitto A, Alpini G, Francis H, Glaser S, et al. Estrogens and the pathophysiology of the biliary tree. World J Gastroenterol. 2006; 12:3537–3545. [PubMed: 16773710]
10. Klein RH, Stephens DN, Ho H, Chen JK, Salmans ML, Wang W, Yu Z, et al. Cofactors of LIM Domains Associate with Estrogen Receptor alpha to Regulate the Expression of Noncoding RNA H19 and Corneal Epithelial Progenitor Cell Function. J Biol Chem. 2016; 291:13271–13285. [PubMed: 27129775]
11. Berteaux N, Lottin S, Monte D, Pinte S, Quatannens B, Coll J, Hondermarck H, et al. H19 mRNA-like noncoding RNA promotes breast cancer cell proliferation through positive control by E2F1. J Biol Chem. 2005; 280:29625–29636. [PubMed: 15985428]
12. Lin Y, Xu L, Wei W, Zhang X, Ying R. Long Noncoding RNA H19 in Digestive System Cancers: A Meta-Analysis of Its Association with Pathological Features. Biomed Res Int. 2016; 2016:4863609. [PubMed: 27738631]
13. Basak P, Chatterjee S, Weger S, Bruce MC, Murphy LC, Raouf A. Estrogen regulates luminal progenitor cell differentiation through H19 gene expression. Endocr Relat Cancer. 2015; 22:505–517. [PubMed: 25944846]
14. Sun H, Wang G, Peng Y, Zeng Y, Zhu QN, Li TL, Cai JQ, et al. H19 lncRNA mediates 17beta-estradiol-induced cell proliferation in MCF-7 breast cancer cells. Oncol Rep. 2015; 33:3045–3052. [PubMed: 25846769]
15. Zhang Y, Liu C, Barbier O, Smalling R, Tsuchiya H, Lee S, Delker D, et al. Bcl2 is a critical regulator of bile acid homeostasis by dictating Shp and lncRNA H19 function. Sci Rep. 2016; 6:20559. [PubMed: 26838806]

16. Jing W, Zhu M, Zhang XW, Pan ZY, Gao SS, Zhou H, Qiu SL, et al. The Significance of Long Noncoding RNA H19 in Predicting Progression and Metastasis of Cancers: A Meta-Analysis. Biomed Res Int. 2016; 2016:5902678. [PubMed: 27672656]
17. Ma L, Tian X, Wang F, Zhang Z, Du C, Xie X, Kornmann M, et al. The long noncoding RNA H19 promotes cell proliferation via E2F-1 in pancreatic ductal adenocarcinoma. Cancer Biol Ther. 2016; 17:1051–1061. [PubMed: 27573434]
18. Wang L, Sun Y, Yi J, Wang X, Liang J, Pan Z, Li L, et al. Targeting H19 by lentivirus-mediated RNA interference increases A549 cell migration and invasion. Exp Lung Res. 2016:1–8.
19. Zhang K, Luo Z, Zhang Y, Zhang L, Wu L, Liu L, Yang J, et al. Circulating lncRNA H19 in plasma as a novel biomarker for breast cancer. Cancer Biomark. 2016; 17:187–194. [PubMed: 27540977]
20. Barsyte-Lovejoy D, Lau SK, Boutros PC, Khosravi F, Jurisica I, Andrulis IL, Tsao MS, et al. The c-Myc oncogene directly induces the H19 noncoding RNA by allele-specific binding to potentiate tumorigenesis. Cancer Res. 2006; 66:5330–5337. [PubMed: 16707459]
21. Reich M, Deutschmann K, Sommerfeld A, Klindt C, Kluge S, Kubitz R, Ullmer C, et al. TGR5 is essential for bile acid-dependent cholangiocyte proliferation in vivo and in vitro. Gut. 2016; 65:487–501. [PubMed: 26420419]
22. Studer E, Zhou X, Zhao R, Wang Y, Takabe K, Nagahashi M, Pandak WM, et al. Conjugated bile acids activate the sphingosine-1-phosphate receptor 2 in primary rodent hepatocytes. Hepatology. 2012; 55:267–276. [PubMed: 21932398]
23. Wang Y, Aoki H, Yang J, Peng K, Liu R, Li X, Qiang X, et al. The role of S1PR2 in bile acid-induced cholangiocyte proliferation and cholestasis-induced liver injury in mice. Hepatology. 2017; Epub ahead of print. doi: 10.1002/hep.29076
24. Barosso IR, Zucchetti AE, Boaglio AC, Larocca MC, Taborda DR, Luquita MG, Roma MG, et al. Sequential activation of classic PKC and estrogen receptor alpha is involved in estradiol 17ss-D-glucuronide-induced cholestasis. PLoS One. 2012; 7:e50711. [PubMed: 23209816]
25. Mauad TH, van Nieuwkerk CM, Dingemans KP, Smit JJ, Schinkel AH, Notenboom RG, van den Bergh Weerman MA, et al. Mice with homozygous disruption of the mdr2 P-glycoprotein gene. A novel animal model for studies of nonsuppurative inflammatory cholangitis and hepatocarcinogenesis. Am J Pathol. 1994; 145:1237–1245. [PubMed: 7977654]
26. Zhou M, Learned RM, Rossi SJ, DePaoli AM, Tian H, Ling L. Engineered fibroblast growth factor 19 reduces liver injury and resolves sclerosing cholangitis in Mdr2-deficient mice. Hepatology. 2016; 63:914–929. [PubMed: 26418580]
27. Lammert F, Wang DQ, Hillebrandt S, Geier A, Fickert P, Trauner M, Matern S, et al. Spontaneous cholecysto- and hepatolithiasis in Mdr2−/− mice: a model for low phospholipid-associated cholelithiasis. Hepatology. 2004; 39:117–128. [PubMed: 14752830]
28. Frijters CM, Ottenhoff R, van Wijland MJ, van Nieuwkerk CM, Groen AK, Oude Elferink RP. Regulation of mdr2 P-glycoprotein expression by bile salts. Biochem J. 1997; 321(Pt 2):389–395. [PubMed: 9020871]
29. Hylemon PB, Zhou H, Pandak WM, Ren S, Gil G, Dent P. Bile acids as regulatory molecules. J Lipid Res. 2009; 50:1509–1520. [PubMed: 19346331]
30. Kwong E, Li Y, Hylemon PB, Zhou H. Bile acids and sphingosine-1-phosphate receptor 2 in hepatic lipid metabolism. Acta Pharm Sin B. 2015; 5:151–157. [PubMed: 26579441]
31. Luo L, Schomaker S, Houle C, Aubrecht J, Colangelo JL. Evaluation of serum bile acid profiles as biomarkers of liver injury in rodents. Toxicol Sci. 2014; 137:12–25. [PubMed: 24085190]
32. Baghdasaryan A, Claudel T, Gumhold J, Silbert D, Adorini L, Roda A, Vecchiotti S, et al. Dual farnesoid X receptor/TGR5 agonist INT-767 reduces liver injury in the Mdr2−/− (Abcb4−/−) mouse cholangiopathy model by promoting biliary HCO(−)(3) output. Hepatology. 2011; 54:1303–1312. [PubMed: 22006858]
33. Thomas C, Auwerx J, Schoonjans K. Bile acids and the membrane bile acid receptor TGR5–connecting nutrition and metabolism. Thyroid. 2008; 18:167–174. [PubMed: 18279017]
34. Iempridee T. Long non-coding RNA H19 enhances cell proliferation and anchorage-independent growth of cervical cancer cell lines. Exp Biol Med (Maywood). 2016

35. Henriquez-Hernandez LA, Flores-Morales A, Santana-Farre R, Axelson M, Nilsson P, Norstedt G, Fernandez-Perez L. Role of pituitary hormones on 17alpha-ethinylestradiol-induced cholestasis in rat. J Pharmacol Exp Ther. 2007; 320:695–705. [PubMed: 17108234]

36. Alvaro D, Invernizzi P, Onori P, Franchitto A, De Santis A, Crosignani A, Sferra R, et al. Estrogen receptors in cholangiocytes and the progression of primary biliary cirrhosis. J Hepatol. 2004; 41:905–912. [PubMed: 15645536]

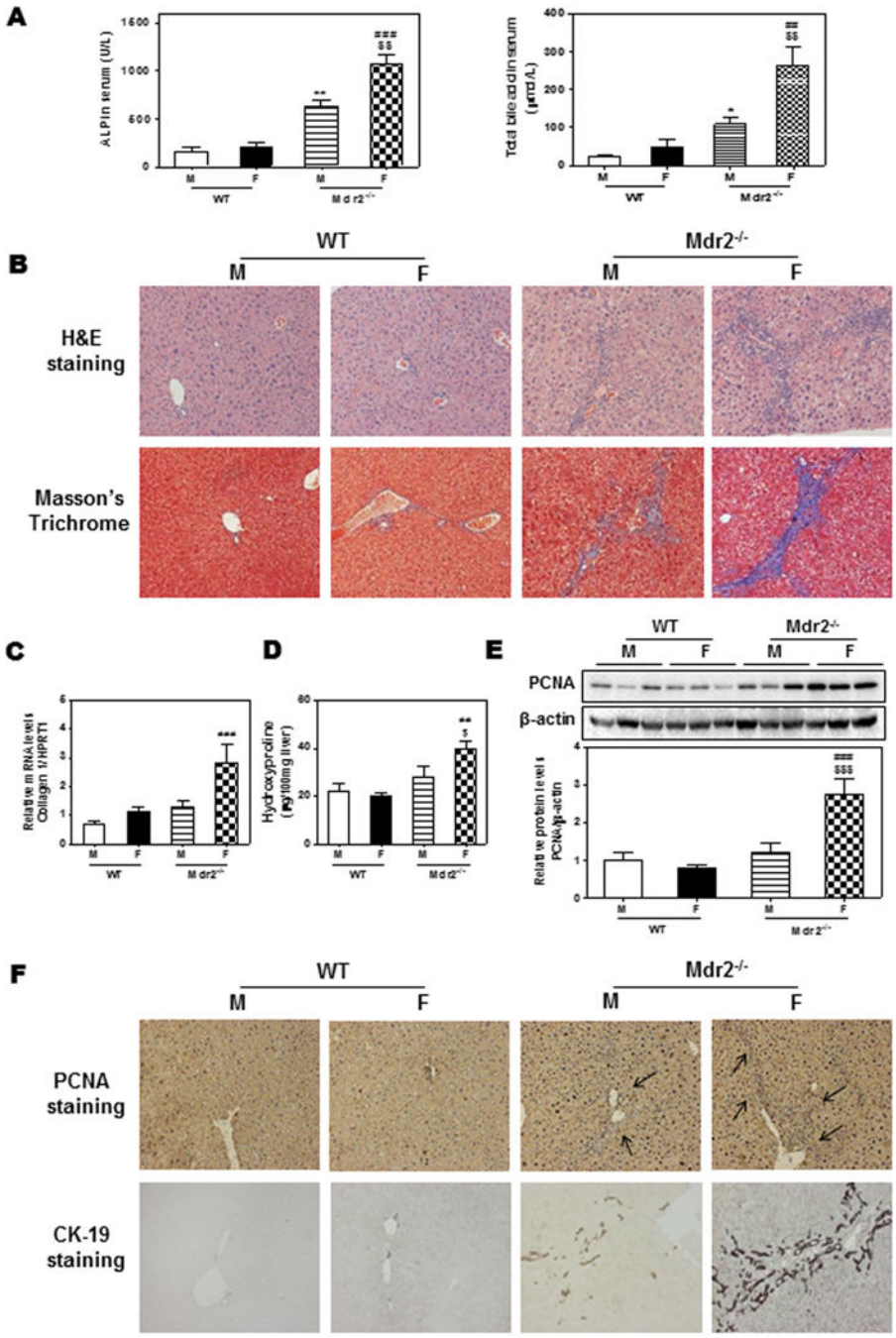

Figure 1. Gender disparity of cholestatic liver injury in Mdr2$^{-/-}$ mice

100-day-old Mdr2$^{-/-}$ mice and age-matched FVB WT mice were sacrificed. (A) Serum levels of ALP and total bile acids (TBA). (B) Representative images of H&E and Masson's Trichrome staining. (C) The mRNA level of collagen I was determined by real-time RT-PCR and normalized using HPRT1 as an internal control. (D) Hepatic hydroxyproline content. (E) Protein level of PCNA was determined by Western blot analysis and normalized with β-actin as an internal control. Representative images are shown. (F) Representative images of immunohistochemistry staining of PCNA and CK-19. Statistical significance: *P< 0.05;

**P<0.01, compared with male (M) WT (WT) mice; ##P<0.01; ###P<0.001, compared with female (F) WT mice; $P < 0.05, $$P<0.01; $$$P<0.001, compared with (M) Mdr2$^{-/-}$ mice (n=6).

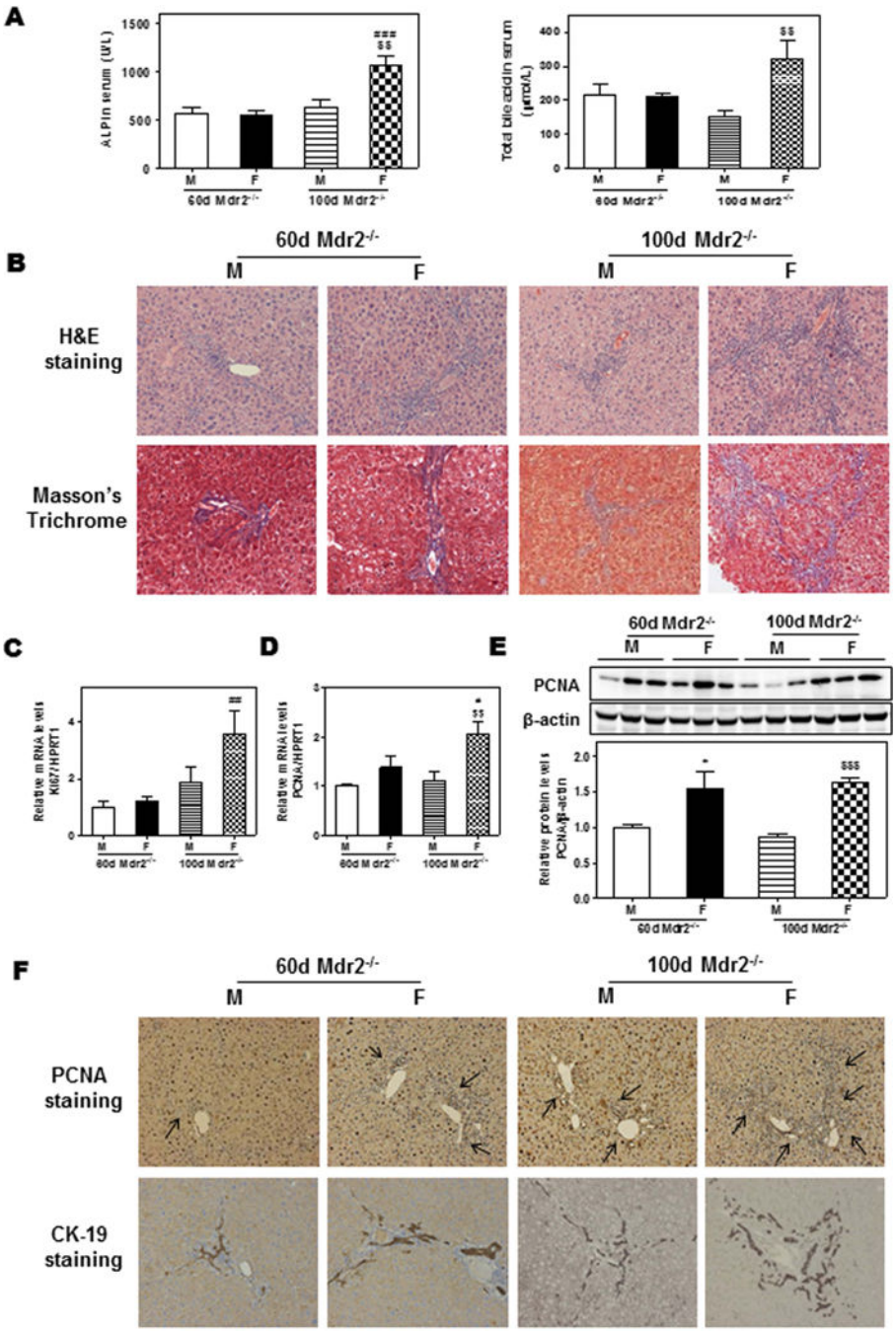

Figure 2. Age disparity of cholestatic liver injury in Mdr2$^{-/-}$ mice

Both male (M) and female (F) Mdr2$^{-/-}$ mice at 60-day and 100-day-old were sacrificed. (A) Serum ALP and TBA levels. (B) Representative images of H&E and Masson's Trichrome staining. (C–D) The relative mRNA levels of Ki67 and PCNA were determined by real-time RT-PCR and normalized using HPRT1. (E) Representative images of Western blot analysis and the relative protein levels of PCNA normalized with β-actin as an internal control. (F) Representative images of immunohistochemical staining of PCNA and CK-19. Statistical significance: *P<0.05, compared with 60-day-old (M) Mdr2$^{-/-}$

mice; $^{\#}P<0.05$, $^{\#\#}P<0.01$, $^{\#\#\#}P<0.001$, compared with 60-day-old (F) $Mdr2^{-/-}$ mice; $^{\$\$}P<0.01$, $^{\$\$\$}P<0.001$, compared with 100-day-old (M) $Mdr2^{-/-}$ mice (n=6).

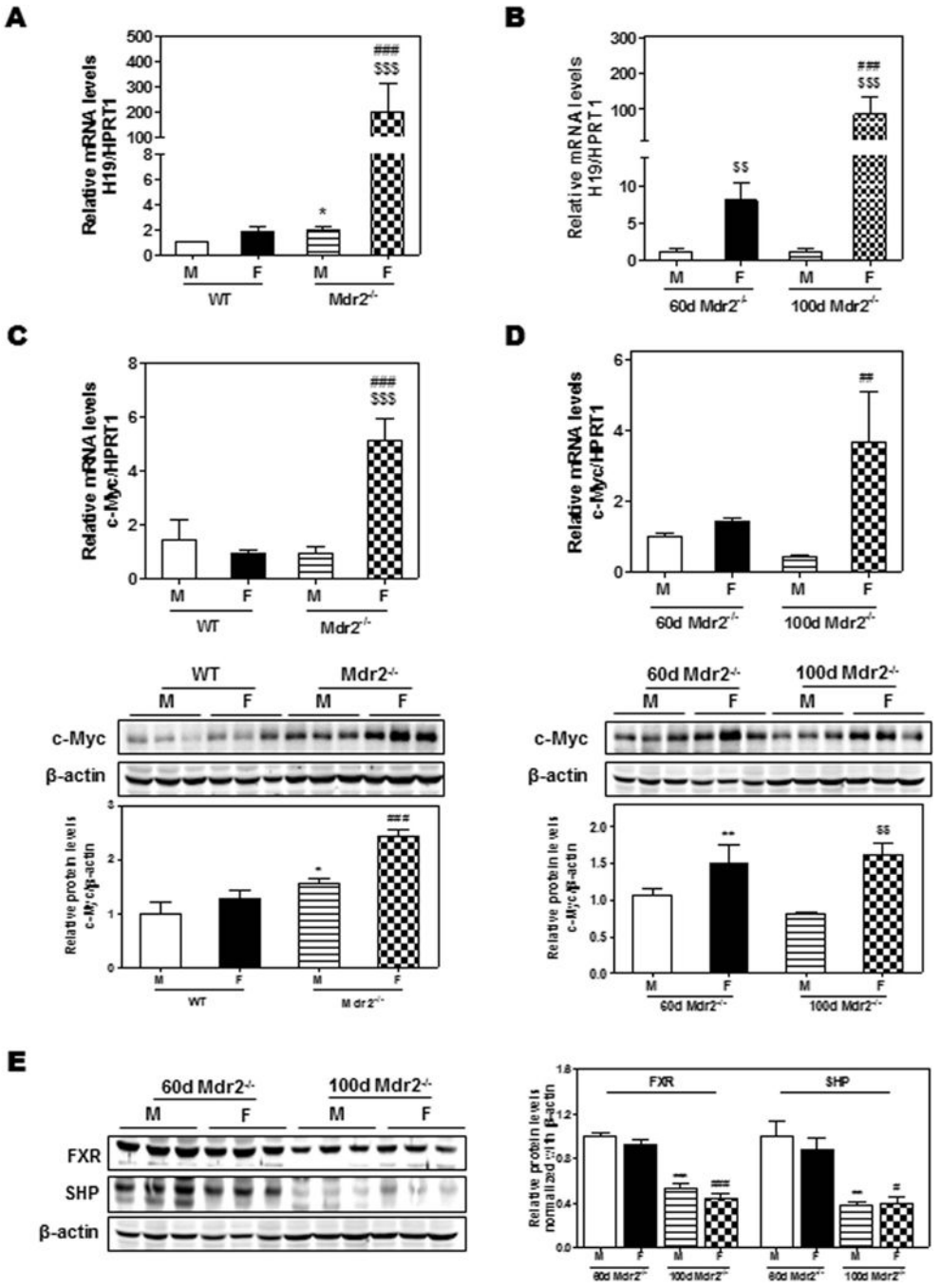

Figure 3. The expression of H19, c-Myc, FXR and SHP in WT and Mdr2$^{-/-}$ mice

(A) H19 expression levels differ in 100-day-old WT and Mdr2$^{-/-}$ mice; (B) H19 expression levels in 60-day-old and 100-day-old Mdr2$^{-/-}$ mice. (C–D) Comparison of the relative mRNA levels and protein expression levels of c-Myc between 100-day-old WT and Mdr2$^{-/-}$ mice (C) and between 60-day-old and 100-day-old Mdr2$^{-/-}$ mice (D); (E) The protein expression levels of FXR and SHP determined by Western blot analysis and normalized with β-actin as an internal control. Statistical significance: *P<0.05, compared with (M) WT

mice; $^{\#\#}$P<0.01, $^{\#\#\#}$P<0.001, compared with (F) WT mice; $^{\$\$}$P<0.01, $^{\$\$\$}$P<0.001, compared with 100-day-old (M) Mdr2$^{-/-}$ mice (n=6).

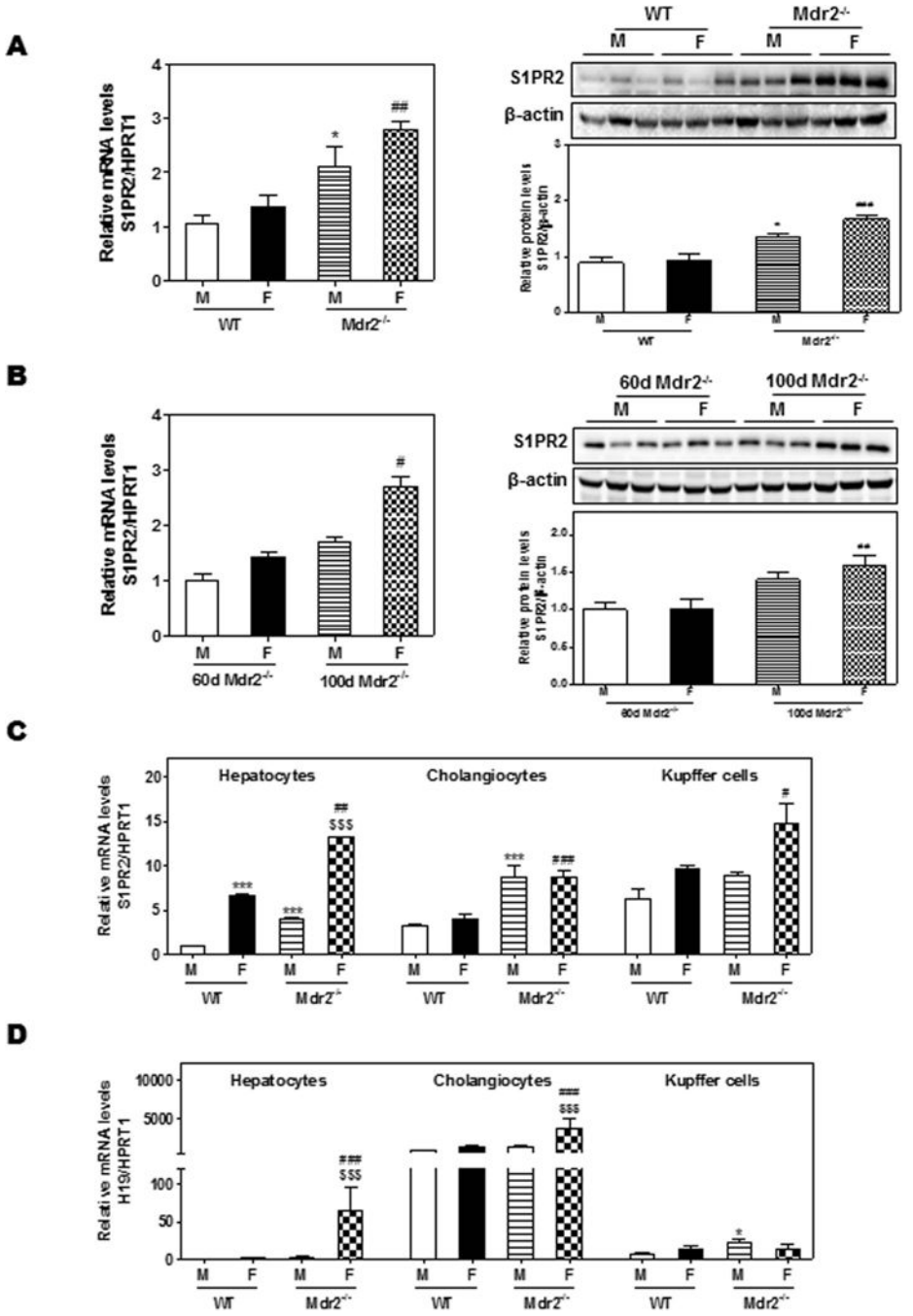

Figure 4. The expression of S1PR2 and H19 in different types of hepatic cells

(A) Comparison of S1PR2 mRNA and protein expression levels between 100-day-old WT and Mdr2$^{-/-}$ mice. (B) Comparison of S1PR2 mRNA and protein expression levels between 60-day and 100-day-old Mdr2$^{-/-}$ mice. (C) Comparison of mRNA expression levels of S1PR2 among primary hepatocytes, cholangiocytes and Kupffer cells isolated from 100-day-old WT and Mdr2$^{-/-}$ mice. Statistical significance: *P<0.05, ***P<0.001, compared with (M) WT mice; $^{\#}$P<0.05, $^{\#\#}$P<0.01, $^{\#\#\#}$P<0.001, compared with (F) WT mice; $^{\$\$\$}$P<0.001, compared with 100-day-old (M) Mdr2$^{-/-}$ mice (n=6)

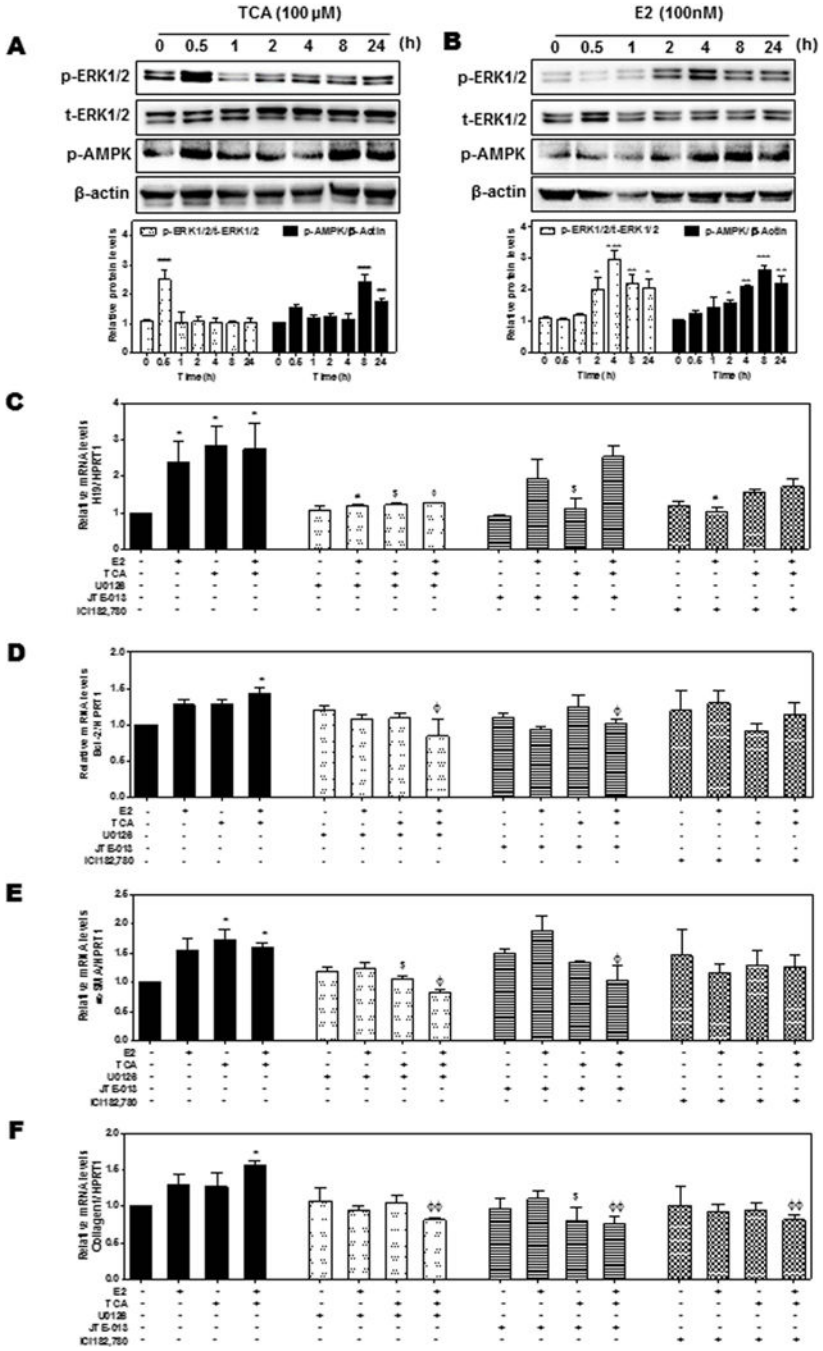

Figure 5. The role of S1PR2 and ERα-mediated ERK1/2 activation in TCA- and E2-mediated expression of H19 and pro-fibrotic genes in cholangiocytes

(A–B) Mouse large cholangiocyte (MLE) cells were treated with a vehicle control, TCA (100 μM) or E2 (100 nM) for 0.5–24 h. The protein levels of phosphorylated ERK1/2 (p-ERK1/2), total ERK1/2 (t-ERK1/2) and p-AMPK were determined by Western blot analysis and normalized with β-actin. Representative immunoblot images are shown. (C–F) MLE cells were pretreated with U0126 (1 μM), JTE-013 (5 μM), ICI182,780 (1 μM) for 1 h, and then treated with vehicle control, TCA (100 μM) or E2 (100 nM) for 48h. The relative expression levels of H19 (C), mRNA levels of Bcl-2 (D), α-SMA (E) and collagen 1 (F)

were determined by real-time RT-PCR and normalized using HPRT1. Statistical significance: *P<0.05, **P <0.01, ***P<0.001, compared with vehicle control group; #P<0.05, compared with E2 group; $P<0.05, compared with TCA group; ΦP<0.05; ΦΦP<0.01, compared wit

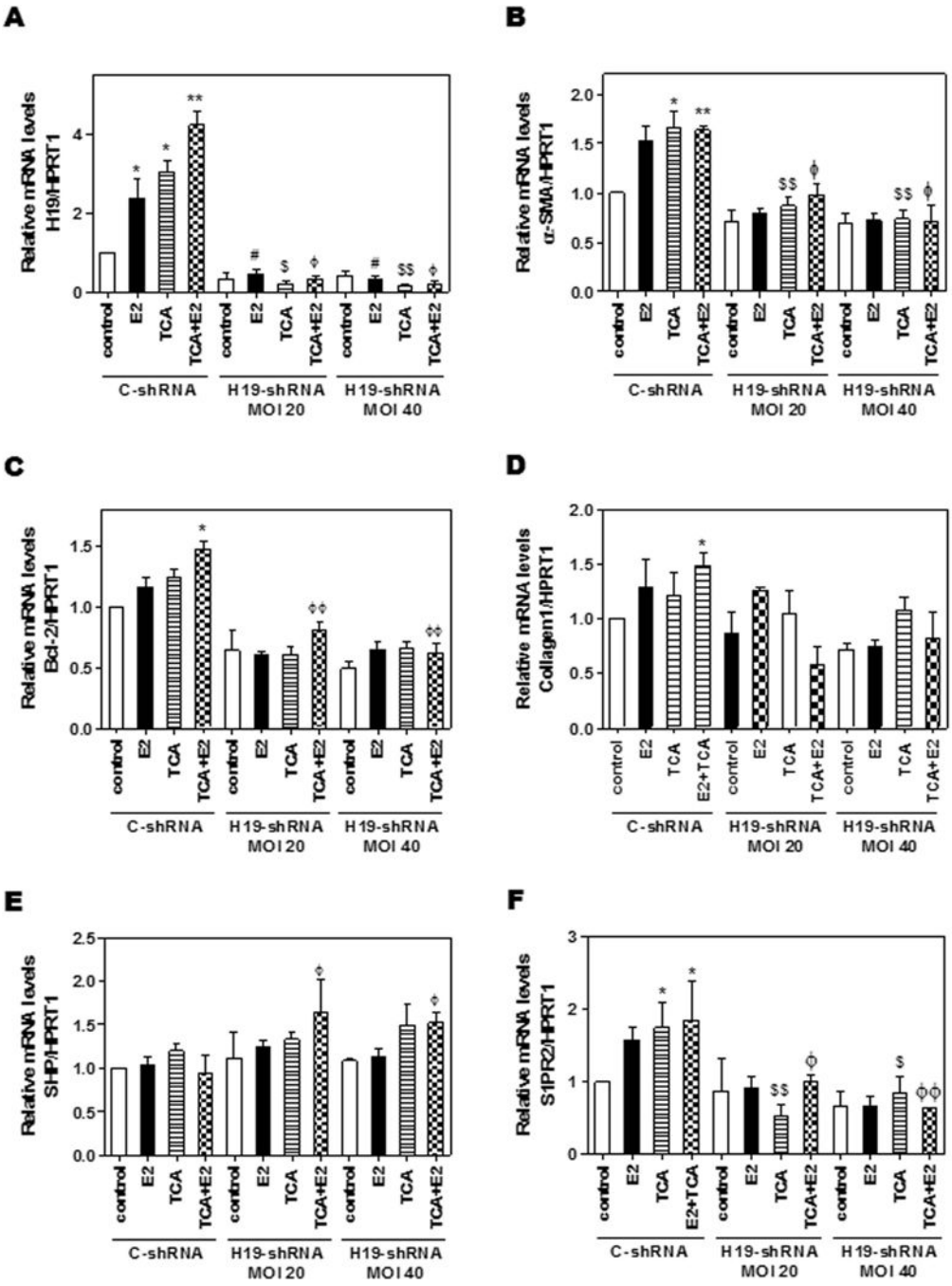

Figure 6. The role of H19 in TCA-/E2-mediated expression of pro-fibrotic genes in cholangiocytes

MLE cells were transduced with control or H19 shRNA adenovirus for 6h before treatment with a vehicle control, TCA (100 μM), E2 (100 nM) or TCA+E2 for 48h. The relative expression levels of H19 (A) and mRNA levels of α-SMA (B), Bcl-2 (C), collagen 1 (D), SHP (E) and S1PR2 (F) were determined by real-time RT-PCR and normalized using HPRT1 as an internal control. Statistical significance: *P<0.05, **P<0.01, compared with vehicle control group; #P<0.05, compared with C-shRNA E2 group; $P<0.05, $$P<0.01,

compared with C-shRNA TCA group; $^{\Phi}P<0.05$, $^{\Phi\Phi}P<0.01$, compared with C-shRNA TCA +E2 group (n=3).

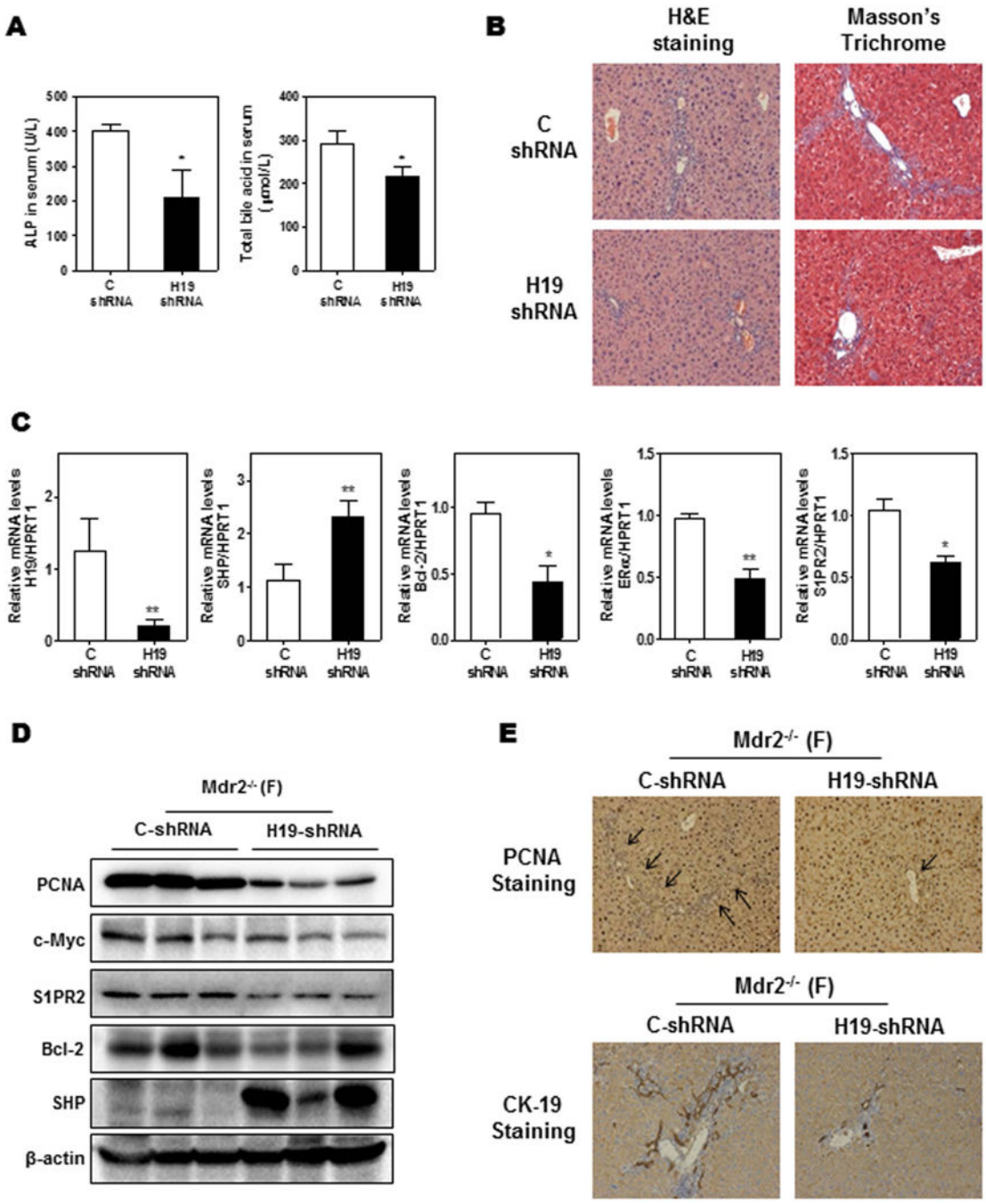

Figure 7. Down-regulation of H19 reduced cholestatic injury in female Mdr2$^{-/-}$ mice

Female (F) Mdr2$^{-/-}$ mice at age 60-day were injected with purified control adenovirus or H19 shRNA adenovirus (2 ×10^{10} virus particles per mouse). Mice were harvested after one week. (A) Serum ALP and TBA levels. (B) Representative images of H&E and Masson's Trichrome staining. (C) The relative mRNA levels of H19, SHP, Bcl-2, ERα and S1PR2 were determined by real-time RT-PCR and normalized using HPRT1. (D) Representative images of Western blot analysis of PCNA, c-Myc, S1PR2, Bcl-2 and SHP normalized with β-actin as an internal control. (E) Representative images of immunohistochemistry staining

of PCNA and CK-19 in livers. Statistical significance: *P<0.05, **P<0.01, compared with control shRNA group (n=6).

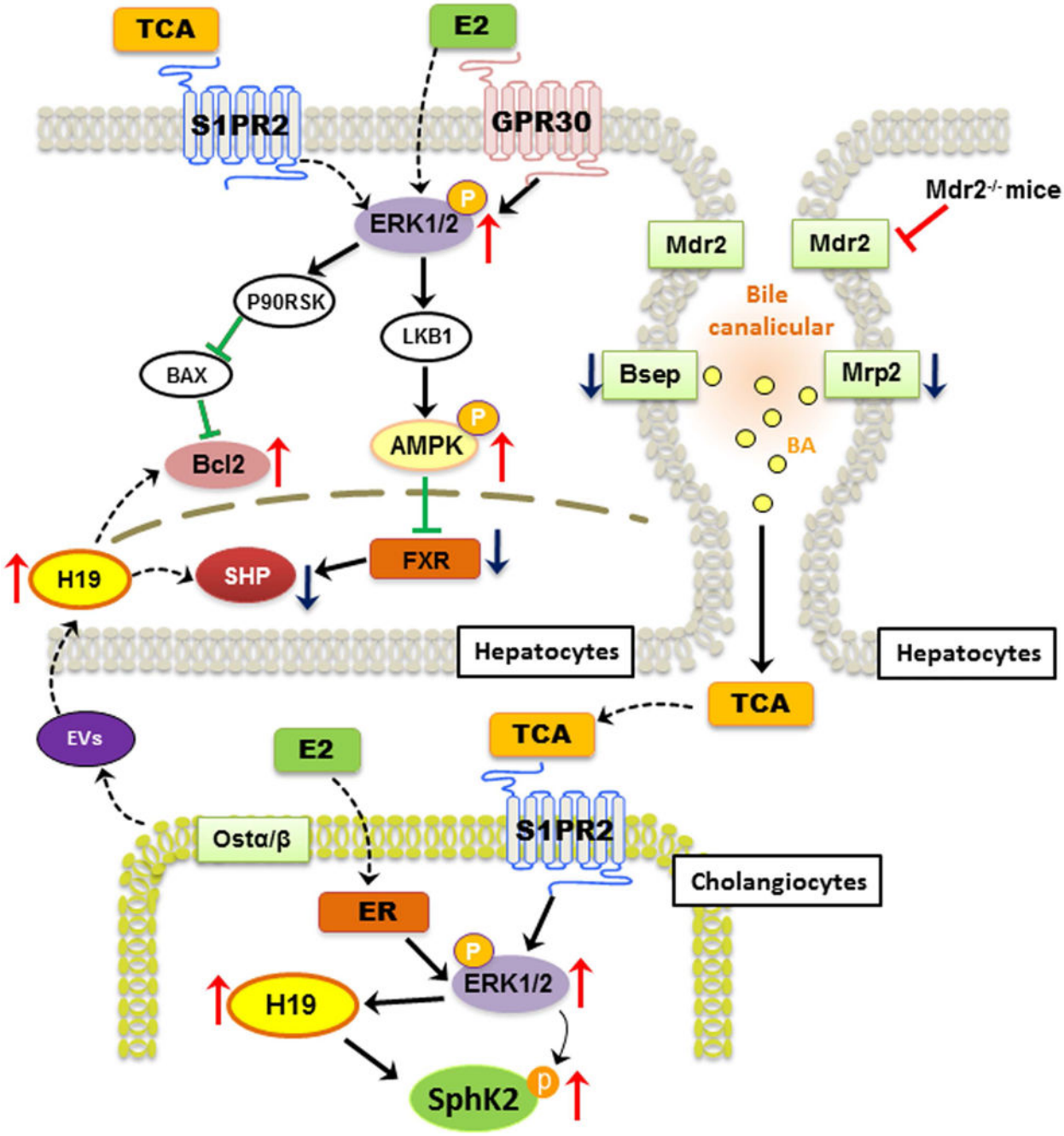

Figure 8. Schematic diagram of potential mechanisms that link bile acid and estrogen with H19-mediated cholestatic injury in female Mdr2$^{-/-}$ mice

TCA-mediated activation of S1PR2 and estrogen-mediated activation of ER further induce activation of ERK1/2 both in cholangiocytes and hepatocytes. In cholangiocytes, both TCA and E2 up-regulate H19 expression, which further increases the expression of pro-fibrotic genes such as c-Myc, collagen I and Bcl-2. In hepatocytes, activation of ERK1/2 further induces phosphorylation of AMPK, which has been shown to inhibit FXR and SHP expression. In addition, the extracellular vesicles (EV) derived from cholangiocytes further downregulate SHP expression and disrupt bile acid homeostasis and ultimately cause hepatic

cholestatic injury. H19 represents a potential candidate marker and a therapeutic target for cholestatic liver injury.